

Research paper

Transdermal delivery of penetrants with differing lipophilicities using *O*-acylmenthol derivatives as penetration enhancersLigang Zhao, Liang Fang ^{*}, Yongnan Xu, Shu Liu, Zhonggui He, Yanyan Zhao

Department of Pharmaceutical Sciences, Shenyang Pharmaceutical University, Shenyang, China

Received 3 August 2007; accepted in revised form 24 October 2007

Available online 1 November 2007

Abstract

To develop more effective compounds as penetration enhancers, *O*-acylmenthol derivatives were synthesized by *l*-menthol and saturated fatty acid, *O*-ethylmenthol (MET), was also synthesized as a reference compound. Their promoting activity on the percutaneous absorption of five model drugs, 5-fluorouracil (5-FU), isosorbide dinitrate (ISDN), lidocaine (LD), ketoprofen (KP), indomethacin (IM), which were selected based on their lipophilicity represented by $\log K_{O/W}$, was tested *in vitro* across full thickness rat skin with each of the evaluated drugs in saturated donor solution. Only 2-isopropyl-5-methylcyclohexyl tetradecanoate (C14 alkyl chain) had promoting effects on the percutaneous permeation of 5-FU; 2-isopropyl-5-methylcyclohexyl hexanoate (C6 alkyl chain), which increased the permeation coefficient (*P*) 1.91-fold, had the highest permeation for ISDN; in the case of LD, the highest increase in *P* was observed with 2-isopropyl-5-methylcyclohexyl heptanoate (C7 alkyl chain), which increased the *P* by 1.58-fold; MET, which increased the *P* by 2.02-fold, provided the best enhancement for KP; 2-isopropyl-5-methylcyclohexyl heptanoate (C7 alkyl chain) produced the highest increase in *P*, 3.70-fold for IM. These results suggest that some newly designed percutaneous absorption enhancers have the potential to enhance drugs with different lipophilicities. A chain length of C6–C10 seemed to be favorable for lipophilic drugs, while C14 was the most effective enhancer for hydrophilic drug (5-FU).

© 2007 Elsevier B.V. All rights reserved.

Keywords: *O*-acylmenthol derivatives; Penetration enhancers; Saturated fatty acid; Percutaneous absorption; Lipophilicity**1. Introduction**

The transdermal route has many advantages for the administration of drugs for local and systemic therapy. However, the outermost layer of skin, the stratum corneum (SC), forms a strong barrier to most exogenous substances including drugs. The barrier function of the SC is attributed to its multilayered wall-like structure, in which terminally differentiated keratin-rich epidermal cells (corneocytes) are embedded in an intercellular lipid-rich matrix [1]. One approach to deliver an effective dose of drug through skin is to reversibly reduce the barrier function of skin with the aid of penetration enhancers or accelerants

[2]. Numerous compounds have been evaluated for penetration enhancing activity, including sulfoxides, laurocapram, pyrrolidones, alcohols and alkanols, glycols, surfactants, and terpenes [3]. Terpenes may offer advantages over such enhancers because of their natural origin as well as generally regarded as safe (GRAS) status [4]. A variety of terpenes, especially the *l*-menthol, have been investigated as enhancers for drugs such as fluorouracil [5], tamoxifen [6], zidovudine [7], morphine hydrochloride [8], and several cardiovascular agents [9]. Recently, considerable attention has been given to *l*-menthol derivatives, and some researchers have synthesized *O*-alkylmenthol and *O*-acylmenthol derivatives, and evaluated their promoting activity on the percutaneous absorption of KP from hydrogel in rats both *in vivo* and *in vitro* [10]. Among these compounds, *O*-ethylmenthol (MET) was most effective and caused relatively little skin irritation. Nakamura et al. [11] evaluated percutaneous absorption of KP from

^{*} Corresponding author. Department of Pharmaceutical Sciences, Shenyang Pharmaceutical University, 103 Wenhua Road, Shenyang, Liaoning 110016, China. Tel./fax: +86 24 23986330.

E-mail address: fangliang2003@yahoo.com (L. Fang).

carboxyvinyl polymer hydrogels in rats *in vivo* and *in vitro*. In the *in vitro* permeation study, at least 2% *l*-menthol was required to obtain the same activity as 0.25% MET. Furthermore, thiomenthol derivatives were synthesized and their enhancing activity on the percutaneous absorption of KP from hydrogels was also evaluated in rats by the same group [12]. Unfortunately, irritation caused by the thiomenthol was almost linearly related to the enhancing activity. Encouraged by the marked enhancing activity of MET, 1-*O*-ethyl-3-*n*-butylcyclohexanol (OEBH) was also synthesized by the same research group [13]. An *in vivo* study in rats showed that the enhancing activity of OEBH was approximately two times higher than MET; however, the skin irritation was almost the same as that of MET. Fuji et al. [14] reported that *l*-Menthoxyp propane-1,2-diol (MPD) had an enhancing effect on indomethacin and antipyrine which was almost three times greater than the control but was less active than the same concentration of *l*-menthol. In conclusion, no synthetic *l*-menthol derivative has exhibited both high enhancing potency and low irritancy; none of the *l*-menthol derivatives has been adopted in clinical situations.

In this study, *l*-menthol was selected as a lead compound to synthesize new types of *O*-acylmenthol derivatives as candidates for percutaneous absorption enhancers. *O*-acylmenthol derivatives have a structure which can be considered to be a chemical combination of menthol and fatty acids, both of which are known to be potent percutaneous absorption enhancers. Both the long alkyl chain moiety and the relative mild polar ring moiety of *O*-acylmenthol seem to be necessary for its action as a penetration promoter. Examination of the effects of these moieties on the action of penetration enhancers, therefore, should give useful information to help with the development of absorption enhancers. There are many factors that influence the effectiveness of penetration enhancers, such as vehicle properties, enhancer concentrations, and the physicochemical properties of the penetrant, however, there are few reports which have dealt systematically with the relationship between the physicochemical properties of the penetrants and the structure–activity of the percutaneous penetration enhancers.

To examine the effectiveness of these enhancers for penetrants having different physicochemical properties, the enhancement of the skin penetration of five drugs with a wide range of *n*-octanol/water partition coefficients by *O*-acylmenthol was examined in this report. In order to further evaluate the effectiveness of the *O*-acylmenthol derivatives, the compound MET was also synthesized as a reference enhancing promoter. The purpose of the present study was to investigate if a correlation exists between the efficacy of the *O*-acylmenthol derivatives with different carbon chain length and model drugs (5-fluorouracil, isosorbide dinitrate, lidocaine, ketoprofen, indomethacin, the physicochemical parameters of these five model drug are presented in Table 1) having different lipophilicities.

Table 1
Physicochemical properties of 5-FU, ISDN, LD, KP, and IM

Parameters	Drugs				
	5-FU	ISDN	LD	KP	IM
Melting point ^a (°C)	282–283	70	68–69	94	160
MW (g mol ^{−1})	130.08	236.14	234.3	254.28	357.8
SP ^b (J cm ^{−3}) ^{1/2}	34.37	27.13	21.57	22.46	21.70
log <i>K</i> _{O/W} ^c	−0.95 ^d	1.34 ^e	2.56 ^f	3.11 ^g	3.80 ^h
PLB ⁱ	9.59	17.58	27.64	28.01	37.34

^a From the Merk index[®].

^b Solubility parameter, calculated by the approaches of Hoftyzer/Van Krevelen [20].

^c *K*_{O/W} is the *n*-octanol/water partition coefficient.

^d [15].

^e [16].

^f [17].

^g [18].

^h [19].

ⁱ Polarizability, calculated using MARVIN[®] software.

2. Materials and methods

2.1. Materials

5-FU, ISDN, LD, KP, and IM were supplied by *Fan-ge Pharmaceutical Co., Ltd.* (Zhejiang, China), *Huangshan Zhonghuang Pharmaceutical Co., Ltd.* (Anhui, China), *Jianglong Pharmaceutical Co., Ltd.* (Shanxi, China), *Zhongdan Pharmaceutical Co., Ltd.* (Jiangsu, China), *Dahongyin Pharmaceutical Co., Ltd.* (Ningbo, China), respectively. Acetaniline, propylparaben and butoben were purchased from *Beijing Xingjin Chemical Plant* (Beijing, China); isopropyl myristate (IPM), acetic acid, propanoic acid, butyric acid, pentanoic acid, hexanoic acid, heptanoic acid, octanoic acid, nonylic acid, decanoic acid, dodecanic acid, tetradecanoic acid, palmitic acid, stearic acid, diethyl sulfate, and *l*-menthol were supplied by *China National Medicines Co., Ltd.* (Shanghai, China); Methanol and acetonitrile of HPLC grade were obtained from the *Yuwang Pharmaceutical Co., Ltd.* (Shandong, China). All other chemicals were of the highest reagent grade available.

2.2. Synthesis of MET and *O*-acylmenthol derivatives

Chemical structures of MET and the synthetic *O*-acylmenthol derivatives are shown in Fig. 1. These compounds were synthesized by two methods. The reaction sequences for the preparation of MET are outlined in Fig. 2a; the reaction sequences for the preparation of *O*-acylmenthol derivatives are outlined in Fig. 2b. The physicochemical parameters of the synthetic enhancers are shown in Table 2. The purity of each compound was over 98% as shown by gas chromatography (GC-14C, Shimadzu, Japan). The structures of the compounds were confirmed by NMR (ARX-300, Bruker, Switzerland) and HPLC-MS (ZQ-2000, Waters, USA). The ¹H NMR and MS data are as follows:

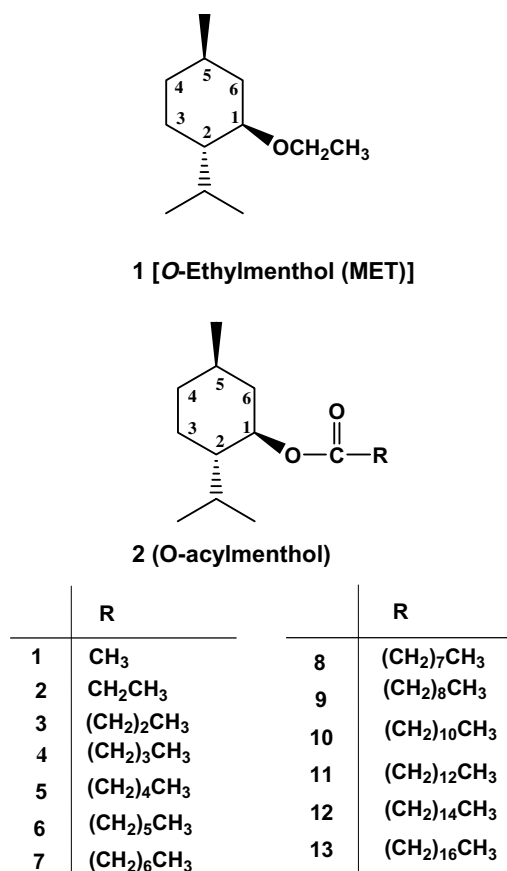


Fig. 1. The chemical structure of MET and *O*-acylmenthol derivatives used as percutaneous absorption enhancers.

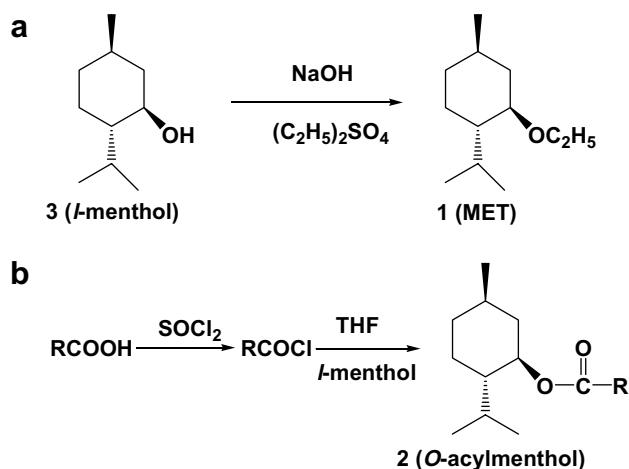


Fig. 2. (a) The reaction sequences for the preparation of MET; (b) the reaction sequences for the preparation of *O*-acylmenthol derivatives.

2.2.1. MET

¹H NMR (CDCl₃), δ : 0.78(3H, d, J = 7.0 Hz, Me-2-isopropyl), 0.86–0.99(8H, m), 1.10–1.50(2H, m), 1.58–1.67(2H, m), 1.9(3H, t, J = 7.0 Hz, Me-ether), 2.06–2.11(1H, m), 2.18–2.23(1H, m), 3.01(1H, sex, J = 4.1 Hz, 10.5 Hz, H-1), 3.33(1H, m, H-6), 3.67(1H, m, H-6); ESI-MS m/z : 184.3 [M^+].

Table 2

Physicochemical properties of IPM, menthol, MET, and *O*-acylmenthol derivatives

Enhancers	Parameters			
	log $K_{O/W}$ ^a	MW (g mol ⁻¹)	SP ^b (J cm ⁻³) ^{1/2}	PLB ^c
IPM	5.61	270.45	16.76	32.82
Menthol	2.78	156.28	20.54	19.05
MET	3.40	184.32	16.63	22.81
M-ACE	2.91	198.3	17.54	22.87
M-PRO	3.54	212.33	17.47	24.71
M-BUT	3.93	226.36	17.41	26.55
M-PEN	4.33	240.38	17.36	28.39
M-HEX	4.73	254.41	17.32	30.24
M-HEP	5.12	268.44	17.28	32.08
M-OCT	5.52	282.46	17.25	33.93
M-NON	5.92	296.49	17.22	35.77
M-DEC	6.31	310.52	17.19	37.62
M-DOD	7.10	338.57	17.15	41.31
M-TET	7.90	366.62	17.12	45.00
M-PAL	8.69	394.67	17.09	48.69
M-STE	9.48	422.73	17.06	52.38

^a Calculated using MARVIN[®] software.

^b Solubility parameter, calculated by approaches of Hoftyzer/Van Krevelen [20].

^c Polarizability, calculated using MARVIN[®] software.

2.2.2. 2-Isopropyl-5-methylcyclohexyl acetate (M-ACE)

¹H NMR (CDCl₃), δ : 0.71(3H, d, J = 7.0 Hz, Me-2-isopropyl), 0.83(3H, d, J = 2.2 Hz, Me-2-isopropyl), 0.85(3H, d, J = 1.6 Hz, Me-5), 0.96–1.05(3H, m), 1.33–1.45(2H, m), 1.73–1.83(2H, m), 1.91–1.94(2H, m), 1.96(3H, s, Me-ester), 4.68(1H, sex, J = 4.4 Hz, 10.8 Hz, H-1); ESI-MS m/z : 198.3 [M^+].

2.2.3. 2-Isopropyl-5-methylcyclohexyl propionate (M-PRO)

¹H NMR (CDCl₃), δ : 0.76(3H, d, J = 7.0 Hz, Me-2-isopropyl), 0.89(3H, d, J = 2.2 Hz, Me-2-isopropyl), 0.91(3H, d, J = 1.6 Hz, Me-5), 0.99–1.04(2H, m), 1.07–1.11(1H, m), 1.14(3H, t, J = 7.6 Hz, Me-ester), 1.33–2.00(6H, m), 2.30(2H, q, J = 7.6 Hz), 4.68(1H, sex, J = 4.4 Hz, 10.8 Hz, H-1); ESI-MS m/z : 212.3 [M^+].

2.2.4. 2-Isopropyl-5-methylcyclohexyl butyrate (M-BUT)

¹H NMR (CDCl₃), δ : 0.76(3H, d, J = 6.9 Hz, Me-2-isopropyl), 0.89(3H, d, J = 2.2 Hz, Me-2-isopropyl), 0.91(3H, d, J = 1.6 Hz, Me-5), 0.97–1.11(6H, m), 1.13–1.15(2H, m), 1.59–1.69(4H, m), 1.83–1.87(1H, m), 1.92–1.98(1H, m), 2.26(2H, t, J = 7.6 Hz), 4.68(1H, sex, J = 4.2 Hz, 10.8 Hz, H-1); ESI-MS m/z : 226.4 [M^+].

2.2.5. 2-Isopropyl-5-methylcyclohexyl pentanoate (M-PEN)

¹H NMR (CDCl₃), δ : 0.76(3H, d, J = 7.0 Hz, Me-2-isopropyl), 0.89(3H, d, J = 2.2 Hz, Me-2-isopropyl), 0.91(3H, d, J = 1.6 Hz, Me-5), 0.92–1.08(6H, m), 1.31–1.41(4H, m), 1.56–1.69(4H, m), 1.85–1.89(1H, m), 1.96–2.02(1H, m), 2.28(2H, t, J = 7.5 Hz), 4.68(1H, sex, J = 4.4 Hz, 10.8 Hz, H-1); ESI-MS m/z : 240.4 [M^+].

2.2.6. 2-Isopropyl-5-methylcyclohexyl hexanoate (*M-HEX*)

^1H NMR (CDCl_3), δ : 0.76(3H, d, $J = 7.0$ Hz, Me-2-isopropyl), 0.89(3H, d, $J = 2.5$ Hz, Me-2-isopropyl), 0.91(3H, d, $J = 1.9$ Hz, Me-5), 0.90–1.11(6H, m), 1.26–1.41(5H, m), 1.49–1.60(1H, m), 1.62–1.69(4H, m), 1.84–1.89(1H, m), 2.27(2H, t, $J = 7.5$ Hz), 4.68(1H, sex, $J = 4.2$ Hz, 10.8 Hz, H-1); ESI-MS m/z : 254.4 $[\text{M}^+]$.

2.2.7. 2-Isopropyl-5-methylcyclohexyl heptanoate (*M-HEP*)

^1H NMR (CDCl_3), δ : 0.77(3H, d, $J = 7.0$ Hz, Me-2-isopropyl), 0.90(3H, d, $J = 2.2$ Hz, Me-2-isopropyl), 0.92(3H, d, $J = 1.8$ Hz, Me-5), 0.90–1.11(7H, m), 1.31–1.40(6H, m), 1.58–1.70(5H, m), 1.85–2.03(2H, m), 2.29(2H, t, $J = 7.4$ Hz), 4.69(1H, sex, $J = 4.3$ Hz, 10.8 Hz, H-1); ESI-MS m/z : 268.4 $[\text{M}^+]$.

2.2.8. 2-Isopropyl-5-methylcyclohexyl octanoate (*M-OCT*)

^1H NMR (CDCl_3), δ : 0.76(3H, d, $J = 6.9$ Hz, Me-2-isopropyl), 0.88(3H, d, $J = 2.3$ Hz, Me-2-isopropyl), 0.91(3H, d, $J = 1.9$ Hz, Me-5), 0.86–1.08(7H, m), 1.28–1.41(8H, m), 1.59–1.69(5H, m), 1.84–2.01(2H, m), 2.29(2H, t, $J = 7.3$ Hz), 4.68(1H, sex, $J = 4.4$ Hz, 10.8 Hz, H-1); ESI-MS m/z : 282.5 $[\text{M}^+]$.

2.2.9. 2-Isopropyl-5-methylcyclohexyl nonanoate (*M-NON*)

^1H NMR (CDCl_3), δ : 0.76(3H, d, $J = 6.9$ Hz, Me-2-isopropyl), 0.89(3H, d, $J = 2.5$ Hz, Me-2-isopropyl), 0.92(3H, d, $J = 1.8$ Hz, Me-5), 0.90–1.11(7H, m), 1.29–1.41(12H, m), 1.60–1.70(4H, m), 1.83–1.97(1H, m), 2.28(2H, t, $J = 7.4$ Hz), 4.68(1H, sex, $J = 4.3$ Hz, 10.8 Hz, H-1); ESI-MS m/z : 296.5 $[\text{M}^+]$.

2.2.10. 2-Isopropyl-5-methylcyclohexyl decanoate (*M-DEC*)

^1H NMR (CDCl_3), δ : 0.77(3H, d, $J = 7.0$ Hz, Me-2-isopropyl), 0.88(3H, d, $J = 2.5$ Hz, Me-2-isopropyl), 0.92(3H, d, $J = 1.9$ Hz, Me-5), 0.90–1.09(7H, m), 1.29–1.38(12H, m), 1.42–1.51(1H, m), 1.60–1.70(5H, m), 1.86–1.89(1H, m), 1.90–2.01(1H, m), 2.29(2H, t, $J = 7.4$ Hz), 4.68(1H, sex, $J = 4.3$ Hz, 10.8 Hz, H-1); ESI-MS m/z : 310.5 $[\text{M}^+]$.

2.2.11. 2-Isopropyl-5-methylcyclohexyl dodecanoate (*M-DOD*)

^1H NMR (CDCl_3), δ : 0.76(3H, d, $J = 6.9$ Hz, Me-2-isopropyl), 0.88(3H, d, $J = 2.6$ Hz, Me-2-isopropyl), 0.92(3H, d, $J = 1.9$ Hz, Me-5), 0.91–1.09(6H, m), 1.26–1.40(16H, m), 1.50–1.69(6H, m), 1.85–2.05(2H, m), 2.27(2H, t, $J = 7.3$ Hz), 4.68(1H, sex, $J = 4.3$ Hz, 10.8 Hz, H-1); ESI-MS m/z : 338.6 $[\text{M}^+]$.

2.2.12. 2-Isopropyl-5-methylcyclohexyl tetradecanoate (*M-TET*)

^1H NMR (CDCl_3), δ : 0.75(3H, d, $J = 7.0$ Hz, Me-2-isopropyl), 0.88(3H, d, $J = 2.6$ Hz, Me-2-isopropyl), 0.91(3H, d, $J = 1.9$ Hz, Me-5), 0.91–1.08(6H, m), 1.26–1.40(20H, m), 1.50–1.69(6H, m), 1.84–2.00(2H, m), 2.27(2H, t, $J = 7.3$ Hz), 4.68 (1H, sex, $J = 4.3$ Hz, 10.7 Hz, H-1); ESI-MS m/z : 366.6 $[\text{M}^+]$.

2.2.13. 2-Isopropyl-5-methylcyclohexyl palmitate (*M-PAL*)

^1H NMR (CDCl_3), δ : 0.75(3H, d, $J = 6.9$ Hz, Me-2-isopropyl), 0.88(3H, d, $J = 2.5$ Hz, Me-2-isopropyl), 0.91(3H, d, $J = 1.9$ Hz, Me-5), 0.91–1.04(6H, m), 1.25–1.3 (22H, m), 1.59–1.69(6H, m), 1.86–2.00(2H, m), 2.27(2H, t, $J = 7.3$ Hz), 4.68(1H, sex, $J = 4.4$ Hz, 10.7 Hz, H-1); ESI-MS m/z : 394.7 $[\text{M}^+]$.

2.2.14. 2-Isopropyl-5-methylcyclohexyl stearate (*M-STE*)

^1H NMR (CDCl_3), δ : 0.75(3H, d, $J = 7.0$ Hz, Me-2-isopropyl), 0.88(3H, d, $J = 2.4$ Hz, Me-2-isopropyl), 0.91(3H, d, $J = 1.9$ Hz, Me-5), 0.93–1.04(6H, m), 1.25–1.39(30H, m), 1.61–1.69(6H, m), 1.87–2.00(2H, m), 2.27(2H, t, $J = 7.4$ Hz), 4.67(1H, sex, $J = 4.4$ Hz, 10.8 Hz, H-1); ESI-MS m/z : 422.7 $[\text{M}^+]$.

2.3. Drug analysis

The HPLC system for analyzing drug concentrations was equipped with an L-2420 variable-wavelength ultraviolet absorbance detector and an L-2130 pump (Hitachi High-Technologies Corporation, Tokyo, Japan). The reversed phase stainless-steel column (20 cm \times 4.6 mm) was packed with Diamonsil C-18 (5 μm particle size; Dikma Technologies, Beijing, China). The HPLC conditions were as follows: the mobile phase of 5-FU consisted of acetonitrile and 0.0364 mol/L monobasic potassium phosphate in distilled water (1:99 v/v), the wavelength was set at 265 nm, and an absolute calibration method was used. The mobile phase of ISDN consisted of methanol and 0.1% acetic acid in distilled water (50:50 v/v), the wavelength was set at 230 nm, and acetanilide was used as internal standard. The mobile phase of LD consisted of methanol, water, acetic acid and triethylamine (62:38:0.3:0.6 v/v), detection was at 230 nm, and acetanilide was used as an internal standard. The mobile phase of KP consisted of methanol and 0.5% acetic acid in distilled water (3:1 v/v), the pH was adjusted to 6.0 with triethylamine, detection was at 260 nm, and butoben was employed as the internal standard. The mobile phase of IM was the same as KP, the wavelength was set at 266 nm, and propylparaben was used as internal standard. The flow rate under the above five conditions was 1.0 ml/min.

2.4. Determination of drug solubility

To determine the saturation solubility of the five drugs in IPM, with and without enhancer, excess drug was added to known volumes of vehicle, vortexed for 2 min followed by sonication for 10 min to dissolve the drug and then equilibrated at 32 ± 0.5 °C for more than 48 h. Finally, the contents were centrifuged at 16,000 rpm for 10 min and aliquots for the supernatant saturated solution were diluted and analyzed by HPLC. The experiments were performed in triplicate.

2.5. Calculation of drug parameters and *O*-acetylmenthol parameters

Five model drugs were selected based on their lipophilicity represented as $\log K_{O/W}$. The physicochemical parameters of the drugs and *O*-acetylmenthol derivatives were obtained from the literature or calculated by MARVIN[®] software; the Hansen solubility parameters of the compounds were calculated from the chemical structures using the approaches of Hoftyzer/Van Krevelen [20]. The calculation of the solubility parameter was based on the average molecular weight. The unit of the solubility parameters is $(\text{J cm}^{-3})^{1/2}$ [21].

2.6. Permeation experiments

2.6.1. Preparation of donor solutions

Donor solutions of the different drugs, including 5-FU, ISDN, LD, KP, and IM, were obtained by equilibration of excess amounts of solute in IPM, with and without selected concentration enhancers, vortexed for 2 min followed by sonication for 10 min to dissolve the drug, and an excess amount of solute was present throughout the experiments.

2.6.2. Skin preparation

Male Wistar rats weighing 180–220 g (6–8 weeks old) used in all experiments were supplied by the Experimental Animal Center of Shenyang Pharmaceutical University (Shenyang, China). All experiments were carried out in accordance with the NIH Guidelines for the Care and Use of Laboratory Animals and also in accordance with the guidelines for animal use published by the Life Science Research Center of Shenyang Pharmaceutical University. All efforts were made to minimize animal suffering and to limit the number of animals used. The rats were anesthetized with urethane (20% w/v, i.p.) and the abdomen was carefully shaved with a razor after removal of hair by electric clippers (model 900, TGC, Japan). Full thickness skin (i.e. epidermis with SC and dermis) was excised from the shaved abdominal site. Any skin which had a disrupted barrier was rejected. After removing the fat and sub-dermal tissue, the skin was kept frozen at -20°C and used within one week. Before starting the experiments, the skin was allowed to reach room temperature for at least 10 h.

2.6.3. Permeation experiments

Skin permeation experiments were performed according to the method of Fang et al. [22]. A diffusion cell consisting of two half-cells with a water jacket connected to a water bath at 32°C was used. Each half-cell had a volume of 2.5 ml and an effective area of 0.95 cm^2 . The dermis side of the skin was in contact with the receiver compartment and the SC with the donor compartment. The donor compartment was filled with the drug suspension and the receiver compartment with pH 7.4 PBS. During all the experiments, excess drug was maintained in the donor compartment. Both donor and receiver compartments

were stirred with a star-head bar driven by a constant speed synchronous motor at 600 rpm. At predetermined time intervals, 2.0 ml of receptor solution was withdrawn from each receiver compartment for analysis and replaced with the same volume of fresh solution to maintain sink conditions. The drug concentration was determined by reversed phase HPLC with reference to a calibration curve.

2.7. Data analysis

The cumulative amount of drugs permeating through the skin was plotted as a function of time. The skin flux was determined from Fick's law of diffusion:

$$J_s = dQ_r / Adt \quad (1)$$

where J_s is the steady-state skin flux in $\mu\text{g}/\text{cm}^2/\text{h}$, dQ_r is the change in quantity of the drug passing through the skin into the receptor compartment in μg , A is the active diffusion area in cm^2 , and dt is the change in time. The flux was calculated from the slope of the linear portion of the profiles. The lag-time was determined by extrapolating the linear portion of the curve to the abscissa [23].

The permeability coefficient (P) was calculated as [24]

$$P = J_s / C_s \quad (2)$$

where C_s is the saturated solubility of drugs in donor solutions.

To evaluate the promoting activity of each enhancer, an enhancing ratio (ER) was defined as follows: $\text{ER} = P$ (with enhancer) / P (without enhancer). Statistical analysis was carried out using analysis of variance (ANOVA), the level of significance was taken as $P < 0.05$. A correlation analysis was performed with the help of the SPSS[®] program, and correlation coefficients were examined for significance ($P < 0.05$) using Student's *t*-test.

3. Results

3.1. Percutaneous absorption of drugs with different *l*-menthol concentrations in vitro

When cumulative amounts permeating as a function of the enhancer concentration were compared at 8 h, a wide fluctuation was apparent. At 5%, 10%, and 20% *l*-menthol levels (w/w), the cumulative transport of 5-FU was 333.59 ± 32.64 , 374.55 ± 19.45 , $259.07 \pm 47.08\text{ }\mu\text{g}/\text{cm}^2$, there is no significant difference with control group which was $416.92 \pm 22.02\text{ }\mu\text{g}/\text{cm}^2$ ($P > 0.05$), also, there was no significant difference among 5%, 10%, and the 20% group ($P > 0.05$), as shown in Fig. 3a, so the 5% level was chosen to perform latter experiment.

As far as the ISDN was concerned, the cumulative amounts of the control group, 5% group, and 10% group were 827.79 ± 40.3 , 827.26 ± 16.3 , and $905.11 \pm 140.3\text{ }\mu\text{g}/\text{cm}^2$, respectively, there was no significant difference among the three ($P > 0.05$). In contrast, the 20% group was

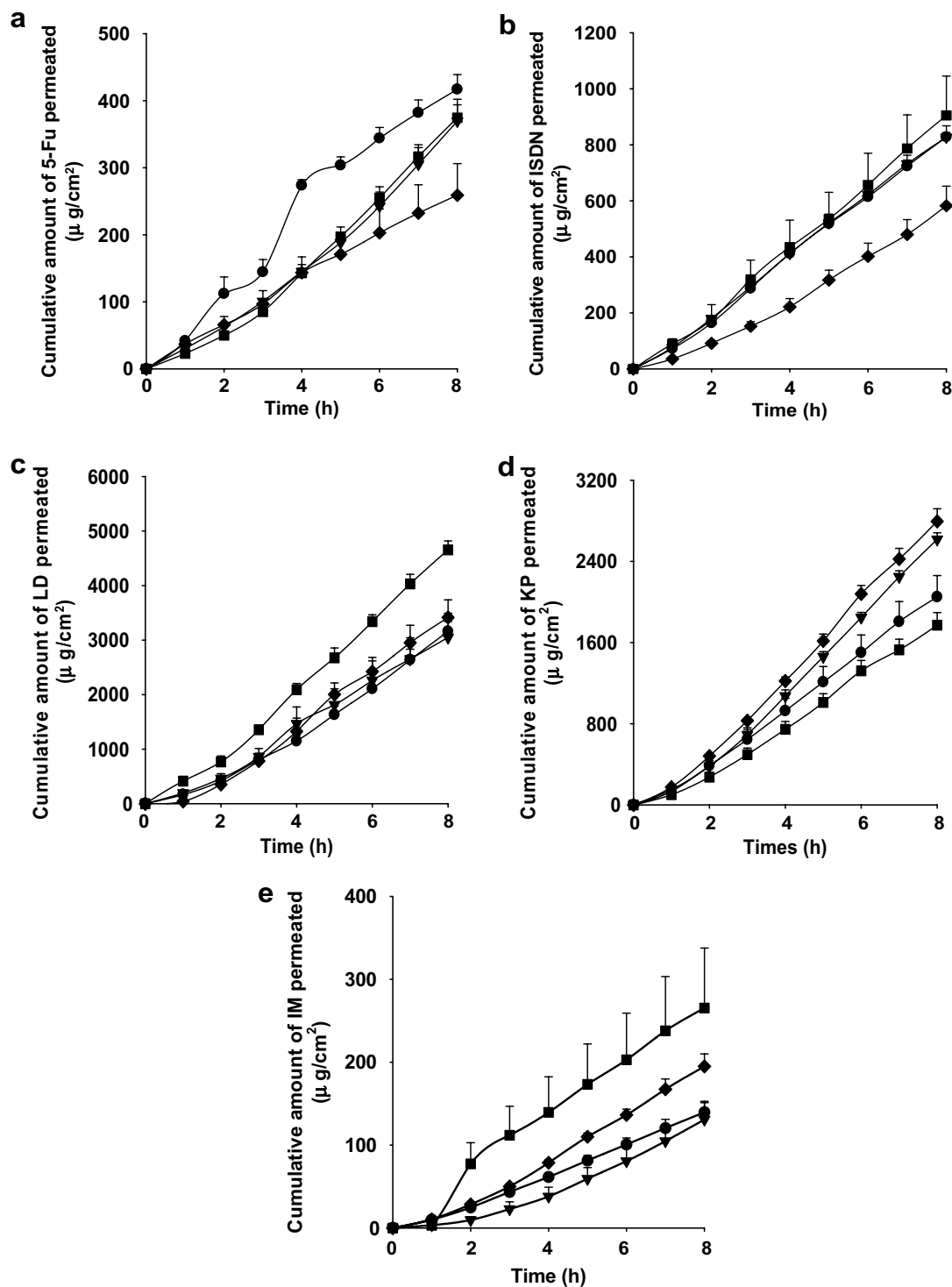


Fig. 3. Permeation profiles of drugs through rat skin (average \pm SE, $n = 4$). Profile (a) is 5-FU; profile (b) is ISDN; profile (c) is LD; profile (d) is KP; profile (e) is IM. Key: (●) menthol concentration is 0%; (▼) menthol concentration is 5%; (■) menthol concentration is 10%; (◆) menthol concentration is 20% (w/w).

$582.65 \pm 69.84 \mu\text{g}/\text{cm}^2$, significantly lower than the control group ($P < 0.05$), as shown in Fig. 3b. Accordingly, 5% was selected as the most suitable concentration for ISDN during subsequent experiments.

At 0%, 5%, and 20% concentrations of *l*-menthol, the cumulative amounts of LD permeated were $3158.87 \pm$

183.28 , 3048.70 ± 443.25 , $3414.77 \pm 323.91 \mu\text{g}/\text{cm}^2$, respectively, there is no significant difference between one another ($P > 0.05$), as shown in Fig. 3c. However, the 10% group was $4655.73 \pm 162.76 \mu\text{g}/\text{cm}^2$, significantly higher than control ($P < 0.05$), and consequently, 10% was chosen for LD to perform subsequent experiments.

At 0%, 5%, and 20% concentrations of *l*-menthol, the cumulative amounts of KP permeated were 2049.63 ± 211.4 , 2617.75 ± 64.73 , and $2795.61 \pm 123.26 \mu\text{g}/\text{cm}^2$, respectively, both 5% and 20% levels were higher than control ($P < 0.05$), while no significant difference was observed between the two ($P > 0.05$). However, the amount of *l*-menthol at 10% led to a reduction which was $1771.02 \pm 125.32 \mu\text{g}/\text{cm}^2$ (Fig. 3d), so 5% level was selected.

Fig. 3e shows the permeation profiles of IM from donor solution containing 0%, 5%, 10%, and 20% *l*-menthol. It can be seen that at 10% concentration, the cumulative permeation of IM was higher than the 20%, 0%, and 5% levels ($P < 0.05$); the permeated amounts of 0%, 5%, 10%, and 20% were $139.55 \pm 22.96 \mu\text{g}/\text{cm}^2$, 130.80 ± 35.22 , 265.36 ± 75.33 , and $194.89 \pm 15.14 \mu\text{g}/\text{cm}^2$, respectively, and therefore, 10% level was chosen to perform latter experiment.

The concentrations of MET and *O*-acylmenthol derivatives during the subsequent experiments were at the same molar concentration with *l*-menthol which was selected for different drugs, respectively.

3.2. Percutaneous absorption of 5-FU in vitro

The effects of MET and *O*-acylmenthol on the percutaneous permeation parameters of 5-FU (solubility, flux, T_{lag} , P , and ER) through rat skin are shown in Table 3. The values for the percutaneous permeation parameters of the 5-FU control group were as follows: $13.14 \mu\text{g}/\text{ml}$ for solubility, $52.25 \pm 3.61 \mu\text{g}/\text{cm}^2$ per h for flux, 0.10 h for the lag-time, and 3.98 ± 0.27 cm per h for P . Almost all the evaluated enhancers had no promoting effects on the percutaneous permeation of 5-FU ($P > 0.05$), except M-TET, relative to the control. It increased the P value by 1.34-fold relative to the control. The highest increase in the Q_8 was also provided by M-TET ($585.63 \pm 28.92 \mu\text{g}/\text{cm}^2$), as shown in Fig. 4a.

3.3. Percutaneous absorption of ISDN in vitro

The effects of MET and *O*-acylmenthol on the percutaneous permeation parameters of ISDN (solubility, flux, T_{lag} , P and ER) through rat skin are presented in Table 3. The control values for ISDN were determined to be $32625.49 \mu\text{g}/\text{ml}$ for the solubility, $107.87 \pm 4.50 \mu\text{g}/\text{cm}^2$ per h for the flux, 0.44 h for the lag-time, and $3.31 \pm 0.14 \times 10^{-3}$ cm per h for P . Most of the evaluated enhancers had effects on the percutaneous permeation of ISDN ($P < 0.05$), except M-ACE, M-BUT, M-PEN, M-DOD, M-TET, and M-STE relative to the control. The highest increase in P was observed with M-HEX, which increased the P by 1.91-fold, followed by M-DEC (1.73-fold), M-OCT (1.51-fold), and M-PAL (1.43-fold). Similar to the ER, M-HEX provided the highest increase in Q_8 ($1395.73 \pm 128.25 \mu\text{g}/\text{cm}^2$), followed by M-PAL ($1233.82 \pm 156.57 \mu\text{g}/\text{cm}^2$) and M-DEC ($1221.43 \pm$

$39.74 \mu\text{g}/\text{cm}^2$), from Fig. 4b. All the enhancers had a longer lag-time relative to the control.

3.4. Percutaneous absorption of LD in vitro

The effects of MET and *O*-acylmenthol on the percutaneous permeation parameters of LD (solubility, flux, T_{lag} , P , and ER) through rat skin are presented in Table 4. The control percutaneous permeation parameters for LD were $171.88 \text{ mg}/\text{ml}$ for the solubility, $502.21 \pm 20.41 \mu\text{g}/\text{cm}^2$ per h for the flux, 1.74 h for the lag-time, $2.92 \pm 0.12 \times 10^{-3}$ cm per h for P . Only had M-HEP and M-OCT effects on the percutaneous permeation of LD relative to the control ($P < 0.05$). The highest increase in P was observed with M-HEP, which increased it by 1.58-fold, followed by M-OCT (1.18-fold). However, M-OCT provided the highest increase in Q_8 ($6239.13 \pm 263.62 \mu\text{g}/\text{cm}^2$) from Fig. 4c, followed by M-HEP ($5683.98 \pm 332.82 \mu\text{g}/\text{cm}^2$) and M-DOD ($5360.30 \pm 684.47 \mu\text{g}/\text{cm}^2$). All the enhancers had a shorter lag-time relative to the control.

3.5. Percutaneous absorption of KP in vitro

The effects of MET and *O*-acylmenthol on the percutaneous permeation parameters of KP (solubility, flux, T_{lag} , P and ER) through rat skin are shown in Table 3. The values for the percutaneous permeation parameters of the KP control group are as follows: $15540.06 \mu\text{g}/\text{ml}$ for the solubility, $284.12 \pm 23.68 \mu\text{g}/\text{cm}^2$ per h for the flux, 0.72 h for the lag-time, and $18.28 \pm 1.52 \times 10^{-3}$ cm per h for P . Most of the enhancers had effects on the percutaneous permeation of KP relative to the control ($P < 0.05$), except M-PEN, M-DEC, M-DOD, M-TET, M-PAL, and M-STE. MET provided the best enhancement activity for KP, it increased the KP in P by 2.02-fold relative to the control, followed by M-PRO (1.87-fold), M-BUT (1.81-fold), M-HEX (1.82-fold), and M-OCT (1.79-fold), no difference was found among these four enhancers ($P > 0.01$). The highest increase in the Q_8 was also provided by MET ($3227.34 \pm 263.79 \mu\text{g}/\text{cm}^2$), the Q_8 of M-PRO, M-HEX, M-OCT, M-NON, M-PAL, and M-STE are almost identical ($P > 0.01$), shown in Fig. 4d.

3.6. Percutaneous absorption of IM in vitro

The effects of MET and *O*-acylmenthol on the percutaneous permeation parameters of IM (solubility, flux, T_{lag} , P and ER) through rat skin are presented in Table 4. The control percutaneous permeation parameters for IM were $1668.84 \mu\text{g}/\text{ml}$ for the solubility, $19.50 \pm 2.37 \mu\text{g}/\text{cm}^2$ per h for the flux, 0.83 h for the lag-time, and $11.68 \pm 1.42 \times 10^{-3}$ cm per h for P . The enhancers which had effects on the percutaneous permeation of IM are M-ACE, M-PRO, M-HEP, M-NON, and M-DEC, relative to the control ($P < 0.05$), while the effects of MET, M-PEN and M-DOD are not significant

Table 3
Permeation parameters of 5-FU, ISDN, and KP through rat abdominal skin

Enhancer	5-FU				ER ^a	ISDN				ER ^a	KP				ER ^a
	Solubility (µg/ml)	Flux (µg/cm ² /h)	T _{lag} (h)	P (cm/h)		Solubility (µg/ml)	Flux (µg/cm ² /h)	T _{lag} (h)	P (cm/h) × 10 ³		Solubility (µg/ml)	Flux (µg/cm ² /h)	T _{lag} (h)	P (cm/h) × 10 ³	
Control	13.14	52.25 ± 3.61	0.10	3.98 ± 0.27	1.00	32625.49	107.87 ± 4.50	0.04	3.31 ± 0.14	1.00	15540.06	284.12 ± 23.68	0.72	18.28 ± 1.52	1.00
5%-M	23.43	47.65 ± 7.65	0.76	2.03 ± 0.33	0.51	33353.27	120.99 ± 13.04	0.44	3.63 ± 0.39	1.10	19488.89	387.62 ± 6.68	1.23	19.89 ± 0.34*	1.09
MET	9.94	39.47 ± 8.60	0.08	3.97 ± 0.86	1.00	32807.21	143.85 ± 8.20	0.16	4.22 ± 0.26*	1.27	12576.95	464.16 ± 38.54	1.02	36.91 ± 3.06*	2.02
M-ACE	14.97	20.63 ± 4.2	0.16	1.38 ± 0.29	0.35	48090.74	78.81 ± 14.76	1.01	1.64 ± 0.31	0.50	12192.50	288.81 ± 11.37	0.26	23.69 ± 0.93*	1.30
M-PRO	16.00	25.47 ± 5.72	0	1.59 ± 0.36	0.40	26982.70	123.31 ± 13.15	1.11	4.57 ± 0.49*	1.38	9550.74	325.68 ± 26.39	0.38	34.10 ± 2.76*	1.87
M-BUT	23.49	21.54 ± 8.14	1.00	0.92 ± 0.35	0.23	29758.31	93.42 ± 7.06	1.07	3.14 ± 0.24	0.95	10373.10	343.39 ± 20.21	1.04	33.10 ± 1.95*	1.81
M-PEN	15.35	26.83 ± 5.61	0.04	1.75 ± 0.37	0.44	30277.81	112.67 ± 4.01	0.74	3.72 ± 0.13	1.12	10933.30	286.83 ± 28.38	1.15	26.23 ± 2.60	1.43
M-HEX	12.31	34.95 ± 3.40	0.19	2.84 ± 0.28	0.71	28872.31	182.67 ± 3.55	0.72	6.33 ± 0.12*	1.91	10541.86	350.08 ± 17.25	1.16	33.21 ± 1.60*	1.82
M-HEP	12.78	32.14 ± 4.54	0.80	2.52 ± 0.36	0.63	29975.73	146.13 ± 16.02	0.48	4.87 ± 0.35*	1.47	9943.94	288.84 ± 10.35	1.15	29.05 ± 1.04*	1.59
M-OCT	25.65	11.39 ± 2.43	0	0.44 ± 0.09	0.11	31933.98	159.27 ± 9.67	0.93	4.99 ± 0.30*	1.51	10649.27	349.16 ± 20.84	1.57	32.79 ± 1.96*	1.79
M-NON	10.26	39.89 ± 6.35	0.49	3.89 ± 0.62	0.98	29722.54	124.66 ± 8.17	0.84	4.19 ± 0.27*	1.27	10600.00	327.25 ± 24.34	0.98	30.87 ± 2.30*	1.69
M-DEC	15.73	33.30 ± 3.02	0.10	2.12 ± 0.19	0.53	28823.60	165.21 ± 5.49	0.43	5.73 ± 0.19*	1.73	11286.06	257.05 ± 16.93	0.67	22.78 ± 1.50	1.25
M-DOD	12.48	26.00 ± 6.42	0.19	2.08 ± 0.51	0.52	35611.63	128.46 ± 12.75	1.74	3.61 ± 0.36	1.09	11112.89	268.19 ± 32.48	0.99	24.13 ± 2.92	1.32
M-TET	14.59	77.75 ± 6.32	0.39	5.33 ± 0.43*	1.34	28738.77	116.40 ± 13.22	0.33	4.05 ± 0.46	1.22	11770.46	298.03 ± 44.01	0.58	25.32 ± 3.74	1.39
M-PAL	12.58	55.38 ± 7.86	0.65	4.40 ± 0.63	1.11	34592.21	163.31 ± 15.29	0.55	4.72 ± 0.44*	1.43	12430.14	307.22 ± 28.62	0.19	24.72 ± 2.30	1.35
M-STE	19.94	16.05 ± 0.82	0	0.81 ± 0.04	0.20	33710.71	111.34 ± 9.42	1.04	3.30 ± 0.27	1.00	12080.29	317.74 ± 28.83	0.18	26.30 ± 2.39	1.44

The receiver phase used an identical pH 7.4 PBS and donor phases consisted of IPM; IPM:Menthol (20:1) (w/w) and equivalent molar *O*-acylmenthol derivatives with menthol in IPM.

Data are given as average ± SE (*n* = 4).

^a ER is the enhancement ratio calculated as follows: ER = *P* (with enhancer)/*P* (without enhancer).

* *P* is significantly different from control group, *P* < 0.05.

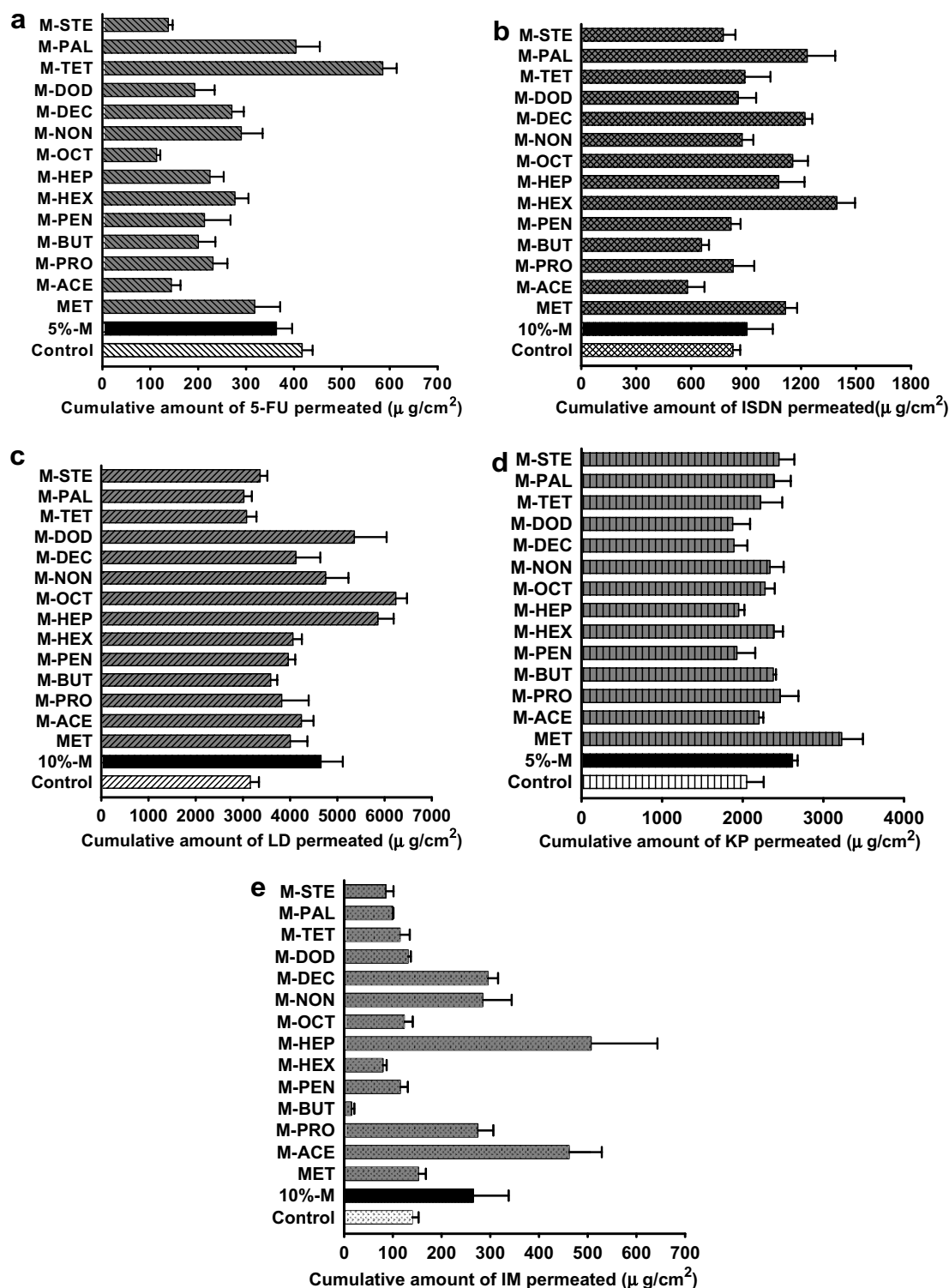


Fig. 4. Cumulative amount (average \pm SE; $n = 4$) of drugs through rat skin, the amount of MET or *O*-acetylmenthol is equal to the molar concentration of menthol in each profile. Profile (a) is 5-FU; profile (b) is ISDN; profile (c) is LD; profile (d) is KP; profile (e) is IM. 5%-M is 5% *L*-menthol in IPM; 10%-M is 10% *L*-menthol in IPM (w/w).

($P > 0.05$). The highest increase in P was observed with M-HEP, which increased it by 3.70-fold relative to the control, followed by M-NON (2.09-fold), M-PRO (2.01-fold), M-ACE (1.97-fold), and M-DEC (1.78-fold), no significant difference of P was observed among these

four enhancers ($P > 0.01$). M-HEP provided the highest increase in Q_8 ($507.05 \pm 137.27 \mu\text{g}/\text{cm}^2$) from Fig. 4e, followed by M-ACE ($461.56 \pm 67.44 \mu\text{g}/\text{cm}^2$). Q_8 of M-PRO, M-NON and M-DEC are not significantly different from one another ($P > 0.05$).

Table 4
Permeation parameters of LD and IM through rat abdominal skin

Enhancer	LD				ER ^a	IM				ER ^a
	Solubility (mg/ml)	Flux (μg/cm ² /h)	T _{lag} (h)	P (cm/h) × 10 ³		Solubility (μg/ml)	Flux (μg/cm ² /h)	T _{lag} (h)	P (cm/h) × 10 ³	
Control	171.88	502.21 ± 20.41	1.74	2.92 ± 0.12	1.00	1668.84	19.50 ± 2.37	0.83	11.68 ± 1.42	1.00
10%-M	264.43	648.46 ± 12.72	0.82	2.45 ± 0.05	0.84	3486.37	31.63 ± 8.11	0	9.07 ± 2.33	0.78
MET	224.83	566.11 ± 24.94	0.93	2.52 ± 0.11	0.86	1610.49	20.57 ± 2.19	0.58	12.77 ± 1.36	1.09
M-ACE	203.65	581.01 ± 15.53	0.80	2.80 ± 0.08	0.96	1829.77	42.14 ± 5.41	0	23.03 ± 2.96*	1.97
M-PRO	168.27	592.68 ± 66.95	1.62	3.52 ± 0.40	1.21	1717.42	40.27 ± 4.21	1.18	23.45 ± 2.45*	2.01
M-BUT	160.07	561.75 ± 43.35	1.57	3.51 ± 0.27	1.20	2482.21	1.52 ± 0.48	0	0.61 ± 0.19	0.05
M-PEN	194.12	509.56 ± 70.03	0.27	2.62 ± 0.36	0.90	1436.81	20.34 ± 3.01	2.41	14.15 ± 2.09	1.21
M-HEX	186.62	544.77 ± 19.02	0.72	2.92 ± 0.10	1.00	1452.35	13.12 ± 0.87	1.96	9.03 ± 0.60	0.77
M-HEP	175.82	810.45 ± 12.71	0.66	4.61 ± 0.07*	1.58	1480.25	63.93 ± 17.01	0.08	43.19 ± 9.49*	3.70
M-OCT	270.18	931.97 ± 39.88	1.34	3.45 ± 0.15*	1.18	2556.82	15.76 ± 1.58	0.16	6.16 ± 0.62	0.53
M-NON	222.94	667.82 ± 61.33	0.83	3.00 ± 0.28	1.03	1533.28	37.38 ± 2.67	0.35	24.38 ± 1.74*	2.09
M-DEC	219.88	606.68 ± 58.96	1.34	2.76 ± 0.27	0.95	2041.28	42.47 ± 2.39	1.00	20.81 ± 1.17*	1.78
M-DOD	216.98	795.85 ± 110.37	1.25	3.67 ± 0.51	1.26	1405.34	18.99 ± 0.98	0.98	13.15 ± 0.70	1.13
M-TET	211.19	443.12 ± 6.00	1.06	2.10 ± 0.03	0.72	1663.65	15.17 ± 1.92	0.51	9.12 ± 1.15	0.78
M-PAL	202.46	420.02 ± 23.11	0.80	2.07 ± 0.11	0.71	1591.92	14.56 ± 0.77	1.29	9.15 ± 0.48	0.78
M-STE	225.27	477.10 ± 44.68	0.89	2.12 ± 0.20	0.73	1605.28	14.05 ± 2.45	1.97	8.75 ± 1.53	0.75

The receiver phase used an identical pH 7.4 PBS and donor phases consisted of IPM; IPM:Menthol (10:1) (w/w) and equivalent molar *O*-acylmenthol derivatives with menthol in IPM. Data are given as average ± SE (*n* = 4).

^a ER is the enhancement ratio calculated as follows: ER = *P* (with enhancer)/*P* (without enhancer).

* *P* is significantly different from control group, *P* < 0.05.

3.7. Correlation analysis results

The correlation analysis using the SPSS® program indicated that the $\log K_{O/W}$ of the drugs exhibited a good correlation with the polarizability of drugs. The Pearson correlation is 0.97 ($P < 0.01$); furthermore, that there was no correlation between solubility and flux nor solubility and P for all the drugs with different lipophilicity. In the case of *O*-acylmenthol derivatives, $\log K_{O/W}$ had a direct correlation with polarizability, the Pearson correlation being 1.00 ($P < 0.01$). Interestingly, the $\log K_{O/W}$ exhibited a negative correlation with the solubility parameters of the derivatives, the Pearson correlation being -0.97 ($P < 0.01$), and there was no correlation between the $\log K_{O/W}$ and flux or P of each drug with a different lipophilicity.

4. Discussion

As the choice of vehicle is one of the important factors in the evaluation of activity for a percutaneous penetration enhancer [25], we evaluated the effect of IPM, a lipophilic vehicle, on the skin permeation of selected drugs with a wide range of lipophilicity ($\log K_{O/W}$, -0.95 – 3.8), in order to further elucidate the effect of *O*-acylmenthol. The solubility parameters of *O*-acylmenthol derivatives were similar to that of IPM (Table 2), which could insure that all the derivatives are fully compatible in IPM and, so, the mixture of derivatives and IPM could also be considered as a lipophilic vehicle. The P is equal to the product of the partition coefficient and the diffusivity of the drug in the membrane divided by the thickness of the membrane (assumed to be relatively constant). The diffusivity of drugs should depend inversely on the cube root of their molar volumes so that the permeability coefficient should not change much, since for many compounds, the MW is often a reasonable approximation of the molecular volume, however, within a narrow range of molecular mass (200–500), there

is little correlation between the size and penetration rate [26]. In the case of the effect of IPM, as shown in Fig. 5a, the experimentally determined permeabilities decreased with increasing drug lipophilicity for a $\log K_{O/W} < 2.56$. These results agreed well with a previous study [27], however, when $\log K_{O/W} > 2.56$, the permeation coefficients increased slightly. The trend in the $\log P$ was similar to the trend in the solubility parameters of the drugs, the Pearson correlation coefficient between the two parameters being 0.91 ($P < 0.05$). At first, as $\log K_{O/W}$ increases, the difference in the solubility parameter between the drug and IPM falls (the drug should become more soluble in IPM) and the $\log P$ values decrease to give an inverse relationship between $\log P$ and $\log K_{O/W}$. Then, as the $\log K_{O/W}$ continues to increase, the distance of solubility parameters between the drugs and solvent becomes larger again (the drug should become more insoluble in IPM), so the $\log P$ value increases. We can conclude that for drugs of a similar size, the greater the difference in the solubility parameter between drug and solvent, the larger the P values that can be obtained from the vehicle. Interestingly, a reverse relationship between the melting point and flux was observed, as shown in Fig. 5b, which agreed well with the report by Izumoto [28]: the lower the melting point, the greater the amount of drug transferred to the skin. This kind of behavior is attributed to the dependence of melting point upon the sum of the energy required to disrupt the crystal [29]. The drug (LD) had the highest flux value, and this phenomenon could have a theoretical explanation. It has been shown theoretically that “hydrophilic” drugs will be enhanced most by agents which have a positive impact on the SC diffusion process. Conversely, “lipophilic” drugs will be transported more efficiently if the enhancer can, in some way, facilitate the SC-viable tissue partitioning step [30]. Some reports [27,31] have shown that when using the lipophilic vehicle IPM, the SC did not seem to offer significant resistance although the viable epidermis

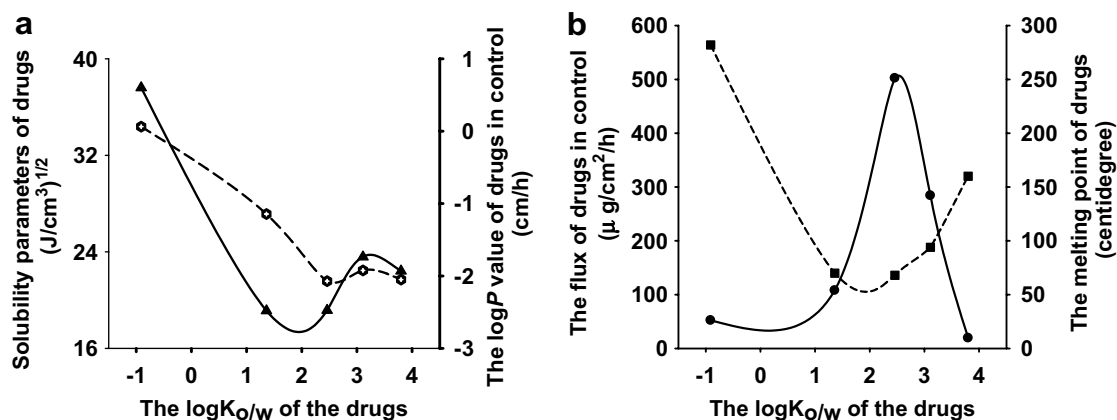


Fig. 5. Graph (a) is the relationship between solubility parameters and permeability of drugs with different lipophilicity from the IPM through rat skin. Graph (b) is the relationship between the melting point and flux of drugs with different lipophilicity from the IPM through rat skin. The data points of flux and permeability represent the mean of four experiments. Key: (○) solubility parameter values; (▲) $\log P$ values; (●) flux values; (■) melting point values. The flux and P values using the parameters are listed in Tables 3 and 4; the $\log K_{O/W}$ and melting point are based on the parameters listed in Table 1.

is the rate-limiting barrier for the transport of relatively hydrophobic drugs, however, LD with the balance of lipophilicity and hydrophilicity [32].

Some researchers hypothesize that if the solubility parameter of the vehicle alters that of the skin so that it is closer to the solubility parameter of the drug, permeation may be enhanced [33]. They found IPM can be permeating into the skin lipids and altering the solubility properties, the degree to which IPM can achieve this will depend on the uptake into the skin and the solubility of caffeine (calculated SP and $\log K_{O/W}$ were $30.7 \text{ (J cm}^{-3})^{1/2}$ and -0.07) which has similar physicochemical property with 5-FU in the modified environment, so this theory may also account for the enhancing activity of IPM for 5-FU. From the information in the literature, it appears that for hydrophilic drugs, such as 5-FU, the primary effect of terpene enhancers is to increase drug diffusivity in the horny layer, i.e. to reduce the barrier properties of the skin [34]. As the promoting effect of IPM focuses on increasing the diffusion coefficient rather than the partition coefficient of the drug, *l*-menthol had no synergistic effects with IPM on 5-FU. However, many reports have shown that terpenes have an enhancing activity on 5-FU in an aqueous vehicle, with or without ethanol [35–37]. Whether *O*-acylmenthol derivatives have a significant promoting activity on 5-FU in relatively polar vehicles needs to be investigated in further studies.

The *O*-acylmenthol derivatives tested exhibited varied enhancing activity for each of the model drugs selected, however, the ER values were relatively low (<4) for both *O*-acylmenthol derivatives and MET. This is a typical observation in penetration enhancement studies: larger effects are much more likely to be observed with penetrants which transport poorly under control conditions. The effect of MET on KP in IPM is not very significant ($ER = 2.02$) compared with its effect on KP in hydrogels (E_r almost equal to 80) [11], this could be due to the fact that IPM also has an enhancing effect.

The solubility parameters of *O*-acylmenthol derivatives were similar to that of IPM, which could insure that all the derivatives are fully compatible in IPM and, so, the mixture of derivatives and IPM with a solubility parameter close to that of the skin $\{ \sim (10 \text{ cal cm}^{-3})^{1/2}$, i.e. $\sim (20.5 \text{ J cm}^{-3})^{1/2} \}$ [33], it might be hypothesized that such vehicles should mix freely with the SC lipid and have maximal enhancement properties. However, significant different activity was observed among the different *O*-acylmenthol derivatives. Similarly, permeants with a solubility parameter close to that of the skin will have a higher permeation rate through the skin, which could elucidate the significantly higher permeation rate of LD and KP than 5-FU and ISDN; the reason for the low flux of IM which also has a solubility parameter close to that of the skin is probably attributed to its high $\log K_{O/W}$ and low water-solubility [38] which makes its partition into the skin lipids more difficult. It is obvious that solubility parameter alone cannot explain the interactions between

the skin membrane and vehicles in all cases. Rather, it is likely that skin membrane flux reflects a combination of different solvent, enhancer and solute characteristics, such as the solubility parameter of solvent, the size and shape of the penetration enhancers, the lipophilicity and water-solubility of the permeants.

In the literature, an optimal chain length has been reported for many enhancers, such as alkyl sulfoxides [39], fatty acids [40], and surfactants [41]. From these reports, a parabolic relationship between the carbon chain length and skin permeation enhancement has been observed. As far as the effect of *O*-acylmenthol on 5-FU is concerned, a similar parabolic behavior was also found (Fig. 6a), meaning that M-TET with a C14 alkyl chain, which was a little different from the literature [42], had the optimal effect and, no matter whether the chain length decreased or increased, the promoting effects were reduced. The *O*-acylmenthol derivatives may act via such a mechanism: In general, the M-TET with polar functional group and a C14 alkyl chain produced the greatest improvement in the absorption of the model hydrophilic permeant 5-FU. This is in agreement with the work of Cornwell and Barry [36] on sesquiterpenes, which also showed that polar functional groups with a relative long chain had improved accelerant activities towards 5-FU. The common feature of ceramides which is the main constituent of SC and providing resistance to chemicals is a relatively small polar head and two long, straight, saturated hydrophobic chains [43]. Because of their structure, M-TET is capable of inserting itself into the lamellae, with their polar head in the polar region and the hydrophobic chain between the hydrophobic chains of the SC lipids. This may induce disturbance of the lipid packing, lateral fluidization of the lamellae and decrease of the skin barrier resistance. Comparison of the structures of M-DOD and M-TET with their activities shows that changing from a C12 tail to a C14 tail markedly improves the enhancing activity. This improvement in activity could possibly be related to the achievement of an ideal carbon chain length [30].

Further structure–activity analysis was carried out by calculation of the $\log K_{O/W}$ of the tested derivatives using the MARVIN[®] software. The relationships between the calculated $\log K_{O/W}$ values and the ER values of different drugs are shown in Fig. 6b–e. As far as the ISDN, LD, KP, and IM were concerned, the straight-chain derivatives from M-ACE to M-STE had different promoting activity sequences compared with 5-FU. Although some different orders also existed among the four lipophilic drugs, it should be noted that the *O*-acylmenthol chain length from C6–C10 provided significant enhancing effects, especially M-HEP produced greatest improvement for IM and LD. However, the reason why M-BUT had a surprisingly low effect on IM is not understood. Since 5-FU is far more hydrophilic than the other four drugs, the addition of *O*-acylmenthol in the IPM system may have a different enhancing mechanism on drugs with a different lipophilicity.

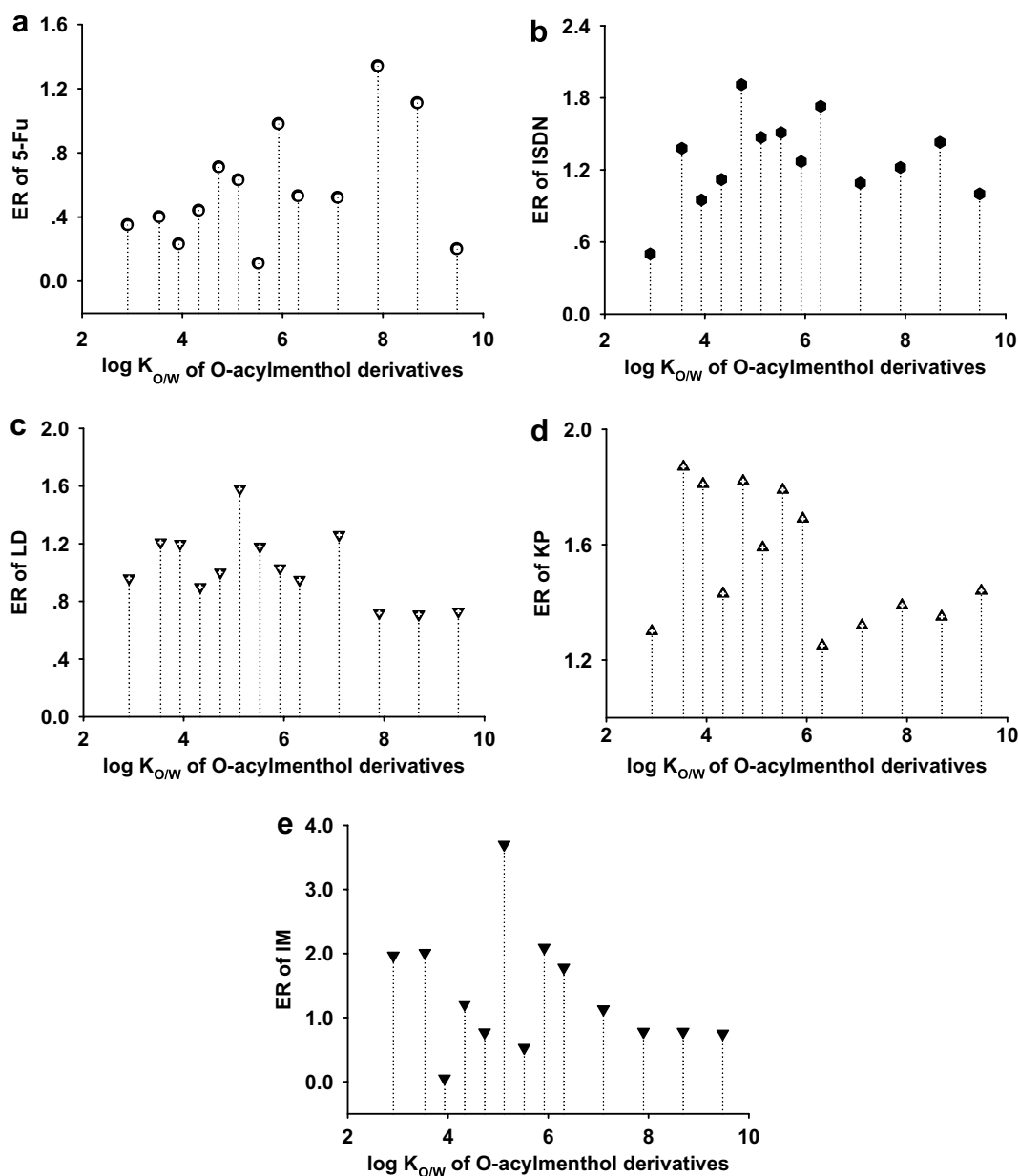


Fig. 6. Relationship between theoretical $\log K_{O/W}$ of *O*-acylmenthol (from M-ACE to M-STE) and ER of drugs with different lipophilicity. Each data point represents the mean of four experiments. Key: (○) ER of 5-FU; (●) ER of ISDN; (▼) ER of LD; (▲) ER of KP; (▼) ER of IM.

As discussed previously, the SC is the main barrier for “hydrophilic” drugs, however, in the case of “lipophilic” drugs, the limiting step for absorption is the lipid (SC)-to-aqueous (viable tissue) partitioning step. Krzysztof Cal et al. [44] reported that both epidermis and dermis can absorb terpenes, while the higher affinity of terpenes for epidermis can be demonstrated, and the amount of terpenes found in the epidermis is over 50% of the total mass. However, Barry [45] reported that the amount of terpenes taken up by the SC ranged from 8.9% to 39%, which suggests that terpene enhancer pooling may occur in the epidermis. In this study, the *O*-acylmenthol derivatives with a chain length from C6–C10 may pool in the epidermis and dermis to reduce the transport of hydrophilic drug

(5-FU) from SC to the acceptor phase. However, this facilitates the permeation of relatively lipophilic drugs (ISDN, LD, KP, and IM). To prove this hypothesis requires further investigation. As ideal skin penetration enhancers are effective, nonirritating, and reversible, the experiments involving irritation tests now in progress will be of importance in assessing enhancer suitability for clinical use.

5. Conclusion

From the results of this investigation, it is concluded that some newly designed percutaneous absorption enhancers synthesized by *l*-menthol and fatty acids have the potential to enhance drugs with different lipophilicity.

The skin permeability of drugs in IPM was related to differences in the solubility parameters between drug and IPM, and there is a reverse relationship between the melting point and flux of the model drug. Furthermore, model drug lipophilicity had a significant impact on the derivative enhancer promoting activity, and a parabolic relationship between flux and $\log K_{O/W}$ of drugs was observed in the IPM. The structure–activity relationships of *O*-acylmenthol derivatives as percutaneous absorption enhancers are summarized as follows: Tail chain length (C2–C18) has important effects on the enhancing activity, C6–C10 seems to be favorable for lipophilic drugs. A parabolic relationship between the carbon chain length of *O*-acylmenthol and skin permeation enhancement has been observed for hydrophilic drug (5-FU), C14 is most effective.

Acknowledgement

The author wishes to thank Professor Yasunori Morimoto, Faculty of Pharmaceutical Sciences, Josai University, Japan, for providing the 2-chamber diffusion cells. The author expresses appreciation to Professor Maosheng Cheng, Faculty of Pharmaceutical Chemistry, Shenyang Pharmaceutical University, China, for providing the MARVIN® software to calculate the parameters of *O*-acylmenthol derivatives.

References

- [1] X. Hui, R.C. Wester, H. Zhai, H.I. Maibach, Chemical partitioning into powdered human stratum corneum: a useful in vitro model for studying interaction of chemicals and human skin, in: R.L. Bronaugh, H.I. Maibach (Eds.), *Percutaneous Absorption*, Taylor & Francis, Boca Raton, 2005, pp. 291–302.
- [2] J. Hadgraft, Passive enhancement strategies in topical and transdermal drug delivery, *Int. J. Pharm.* 184 (1999) 1–6.
- [3] A.C. Williams, B.W. Barry, Penetration enhancers, *Adv. Drug. Dev. Rev.* 56 (2004) 603–618.
- [4] R.A. Thakur, Y. Wang, B.B. Michniak, Essential oils and terpenes, in: E.W. Smith, H.I. Maibach (Eds.), *Percutaneous Penetration Enhancers*, CRC Press, Boca Raton, 2006, pp. 159–173.
- [5] P.A. Cornwell, B.W. Barry, The routes of penetration of ions and 5-fluorouracil across human skin and the mechanisms of action of terpene skin penetration enhancers, *Int. J. Pharm.* 94 (1993) 189–194.
- [6] S. Gao, J. Singh, In vitro percutaneous absorption enhancement of a lipophilic drug tamoxifen by terpenes, *J. Control. Release* 51 (1998) 193–199.
- [7] S. Thomas, K. Narishetty, R. Panchagnula, Transdermal delivery of zidovudine: effect of terpenes and their mechanism of action, *J. Control. Release* 95 (2004) 367–379.
- [8] Y. Morimoto, Y. Wada, T. Seki, In vitro permeation of morphine hydrochloride during the finite application of penetration-enhancing system containing water, ethanol and *l*-menthol, *Biol. Pharm. Bull.* 25 (2002) 134–136.
- [9] D. Kobayashi, T. Matsuzawa, K. Sugibayashi, Feasibility of use of several cardiovascular agents in transdermal therapeutic systems with *l*-menthol–ethanol system on hairless rat and human skin, *Biol. Pharm. Bull.* 16 (1993) 254–258.
- [10] J. Negishi, K. Takayama, K. Higashiyama, Y. Chida, K. Isowa, T. Nagai, Promoting effect of *O*-alkylmenthol and *O*-acylmenthol derivatives on the percutaneous absorption of ketoprofen in rats, *STP Pharma Sci.* 5 (1995) 156–161.
- [11] Y. Nakamura, K. Takayama, K. Higashiyama, T. Suzuki, T. Nagai, Promoting effect of *O*-ethylmenthol on the percutaneous absorption of ketoprofen, *Int. J. Pharm.* 145 (1996) 29–36.
- [12] Y. Takanashi, K. Higashiyama, H. Komiya, K. Takayama, T. Nagai, Thiomenthol derivatives as novel percutaneous absorption enhancers, *Drug Dev. Ind. Pharm.* 25 (1999) 89–94.
- [13] Y. Obata, C.J. Li, M. Fujikawa, K. Takayama, H. Sato, K. Higashiyama, T. Nagai, Evaluation and structure–activity relationship of synthesized cyclohexanol derivatives on percutaneous absorption of ketoprofen using artificial neural network, *Int. J. Pharm.* 212 (2001) 223–231.
- [14] M. Fuji, Y. Takeda, M. Yoshida, N. Utoguchi, M. Matsumoto, Y. Watanabe, Comparison of skin permeation enhancement by 3-*l*-menthoxypropane-1,2-diol and *l*-menthol: the permeation of indomethacin and antipyrine through Yucatan micropig skin and changes in infrared spectra and X-ray diffraction patterns of stratum corneum, *Int. J. Pharm.* 258 (2003) 217–233.
- [15] J. Kirschbaum, High-pressure liquid chromatography of triamcinolone acetate: effect of different octadecylsilane columns on mobility, *J. Pharm. Sci.* 69 (1980) 481–482.
- [16] G.F. Li, Y.S. Quan, K.Y. Fumio, Influence of different layers of skin on the percutaneous absorption of drugs with different lipophilicity, *Chin. Pharm. J.* 37 (2002) 833–836.
- [17] G.R. Strichartz, Fundamental properties of local anesthetic II measured octanol:buffer partition coefficients and pK_a values of clinical used drugs, *Anesth. Analg.* 71 (1990) 58–70.
- [18] Y. Morimoto, Prediction of skin permeability of drugs: comparison of human and hairless rat skin, *J. Pharm. Pharmacol.* 44 (1992) 634–639.
- [19] H.P. Deppeler, Hydrochlorothiazide, in: K. Florey (Ed.), *Analytical profiles of drug substances*, Academic press, New York, pp. 443–469.
- [20] V. Krevelen, D.W. Krevelen, *Properties of Polymers*, Elsevier, Sci. Publ. Co., Amsterdam, 1990.
- [21] B.C. Hancock, P. York, R.C. Rowe, The use of solubility parameters in pharmaceutical solid dosage form design, *Int. J. Pharm.* 148 (1997) 1–21.
- [22] L. Fang, Y. Kobayashi, S. Numajiri, D. Kobayashi, K. Sugibayashi, Y. Morimoto, The enhancing effect of a triethanolamine-ethanol-isopropyl myristate mixed system on the skin permeation of acidic drugs, *Biol. Pharm. Bull.* 25 (2002) 1339–1344.
- [23] E.M. Niazy, Differences in penetration-enhancing effect of Azone through excised rabbit, rat, hairless mouse, guinea pig and human skins, *Int. J. Pharm.* 130 (1996) 225–230.
- [24] R.J. Scheuplein, Site variations in diffusion and permeability, in: A. Jarret (Ed.), *The Physiology and Pathophysiology of Skin*, Academic Press, New York, 1978, pp. 1693–1730.
- [25] N.V. Sheth, D.J. Freeman, W.I. Higuchi, S.L. Spruance, The influence of Azone, propylene glycol and polyethylene glycol on in vitro skin penetration of trifluorothymidine, *Int. J. Pharm.* 28 (1986) 201–209.
- [26] R.H. Guy, J. Hadgraft, Transdermal drug delivery: a simplified pharmacokinetic approach, *Int. J. Pharm.* 24 (1985) 267–274.
- [27] L. Fang, S. Numajiri, D. Kobayashi, Y. Morimoto, The use of complexation with alkanolamines to facilitate skin permeation of mefenamic acid, *Int. J. Pharm.* 262 (2003) 13–22.
- [28] T. Izumoto, A. Aioi, S. Uenoyama, S. Kuriyama, Relationship between the transference of a drug from a transdermal patch and the physicochemical properties, *Chem. Pharm. Bull.* 40 (1992) 456–458.
- [29] L.M. Monene, C. Goosen, J.C. Breytenbach, J. Hadgraft, Percutaneous absorption of cyclizine and its alkyl analogues, *Eur. J. Pharm. Sci.* 24 (2005) 239–244.
- [30] M. Hori, S. Satoh, H.I. Maibach, R.H. Guy, Enhancement of propranolol hydrochloride and diazepam skin absorption in vitro: effect of enhancer lipophilicity, *J. Pharm. Sci.* 80 (1991) 32–35.
- [31] B.P. Wenkers, B.C. Lippold, Skin penetration of non-steroidal anti-inflammatory drugs out of a lipophilic vehicle: influence of the viable epidermis, *J. Pharm. Sci.* 88 (1999) 1326–1331.

- [32] A.C. Williams, B.W. Barry, Terpenes and the lipid–protein-partitioning theory of skin penetration enhancement, *Pharm. Res.* 8 (1991) 17–24.
- [33] M. Dias, J. Hadgraft, M.E. Lane, Influence of membrane–solvent–solute interactions on solute permeation in skin, *Int. J. Pharm.* 340 (2007) 65–70.
- [34] A. Brodin, A. Nyqvist-mayer, T. Wadsten, Phase diagram and aqueous solubility of lidocaine-prilocaine binary system, *J. Pharm. Sci.* 73 (1984) 481–484.
- [35] S. Gao, J. Singh, Mechanism of transdermal transport of 5-fluorouracil by terpenes: carvone, 1, 8-cineole and thymol, *Int. J. Pharm.* 154 (1997) 67–77.
- [36] P.A. Cornwell, B.W. Barry, Sesquiterpene components of volatile oils as skin penetration enhancers for the hydrophilic permeant 5-fluorouracil, *J. Pharm. Pharmacol.* 46 (1994) 261–269.
- [37] H. Okamoto, M. Ohyabu, M. Hashida, H. Sezaki, Enhanced penetration of mitomycin C through hairless mouse and rat skin by enhancers with terpene moieties, *J. Pharm. Pharmacol.* 39 (1987) 531–534.
- [38] Z. Liron, S. Cohen, Percutaneous absorption of alkanolic acids II: application of regular solution theory, *J. Pharm. Sci.* 73 (1984) 538–542.
- [39] D.L. Sekura, S. James, The percutaneous absorption of alkyl methyl sulfoxides, *Adv. Biol. Skin* 12 (1972) 257–269.
- [40] E.R. Cooper, Increased skin permeability for lipophilic molecules, *J. Pharm. Sci.* 73 (1984) 1153–1156.
- [41] N. Kanikkannan, K. Kandimalla, S.S. Lamba, M. Singh, Structure–activity relationship of chemical penetration enhancers in transdermal drug delivery, *Curr. Med. Chem.* 7 (2000) 593–608.
- [42] K.A. Walters, O.J. Olejnik, Effects of nonionic surfactants on the hairless mouse skin penetration of methyl nicotinate, *J. Pharm. Pharmacol.* 35 (1983) 79.
- [43] S.T. Marjukkan, J.A. Bouwstra, A. Urtti, Chemical enhancement of percutaneous absorption in relation to stratum corneum structural alterations, *J. Control. Release* 59 (1999) 149–161.
- [44] K. Cal, S. Janicki, M. Sznitowska, In vitro studies on penetration of terpenes from matrix-type transdermal systems through human skin, *Int. J. Pharm.* 224 (2001) 81–88.
- [45] P.A. Cornwell, B.W. Barry, J.A. Bouwstra, G.S. Gooris, Modes of action of terpene penetration enhancers in human skin; differential scanning calorimetry, small-angle X-ray diffraction and enhancer uptake studies, *Int. J. Pharm.* 127 (1996) 9–26.